



International Journal of Information and Communication Technology

ISSN online: 1741-8070 - ISSN print: 1466-6642

<https://www.inderscience.com/ijict>

Automatic separation robot system of insulated optical units of OPGW optical cable combined with machine vision

Yong Wei, Wenzhao Liu, Jiaju Zhang, Xiaofan Su, Feng Chen

Article History:

Received:	18 July 2024
Last revised:	28 October 2024
Accepted:	28 October 2024
Published online:	13 February 2025

Automatic separation robot system of insulated optical units of OPGW optical cable combined with machine vision

Yong Wei, Wenzhao Liu and Jiaju Zhang*

State Grid Hebei Electric Power Company Co. Ltd.
Information and Telecommunication Branch,
Shijiazhuang, China
Email: 13398618998@163.com
Email: 296899050@qq.com
Email: zjiaz0@126.com
*Corresponding author

Xiaofan Su

R&D of Fiber Optic Cable,
Yangtze Optical Fibre and Cable Joint Stock Limited Company,
Wuhan, Hubei, China
Email: suxiaofan@yofc.com

Feng Chen

Design and Manufacturing of Fiber Optic Cable,
Yangtze Optical Fibre and Cable Joint Stock Limited Company,
Wuhan, Hubei, China
Email: chenfeng_cab@yofc.com

Abstract: This paper aims to integrate machine vision into intelligent robots to realise the automatic separation of insulated optical units of OPGW optical cables. This paper combines improved machine vision to construct a three-dimensional space model of OPGW optical cable, and combines three-dimensional measurement technology to identify the insulated optical units from the optical cable structure. The experimental results show that the operation effect of the system is very remarkable, the three-dimensional coordinate guided mechanical finger point accuracy measured by this binocular system reached 0.4 mm, and the maximum radial and axial loads of the tool were within the rated load, which indirectly demonstrates the feasibility of this method and structural design. The robot system designed in this article reduces the damage to the metal layer of cables caused by traditional methods, lowers the risk of cable stripping. It also provides automation reference for more complex cable operations in the future.

Keywords: machine vision; insulated optical unit of optical cable; automatic separation; robot.

Reference to this paper should be made as follows: Wei, Y., Liu, W., Zhang, J., Su, X. and Chen, F. (2025) ‘Automatic separation robot system of insulated optical units of OPGW optical cable combined with machine vision’, *Int. J. Information and Communication Technology*, Vol. 26, No. 3, pp.25–46.

Biographical notes: Yong Wei graduated from North China Electric Power University with a Bachelor’s in Communication Engineering and Master’s in Project Management from North China Electric Power University. He is a Senior Engineer of the Information and Communication Branch of State Grid Hebei Electric Power Co., Ltd. and a model worker of State Grid Corporation of China. He is currently engaged in power communication construction and management.

Wenzhao Liu is an intermediate engineer and he is a young pioneer of State Grid Hebei Electric Power Company Co. Ltd. Informatica and Telecommunication Branch. He has been engaged in the construction and management of power communication engineering for a long time.

Jiaju Zhang is a senior engineer and he is a young pioneer of State Grid Hebei Electric Power Company. He has been engaged in the construction and management of power communication engineering for a long time.

Xiaofan Su received his BS and ME in Material Processing Engineering in Northwestern Polytechnical University, China in 2009. He joined the Yangtze Optical Fibre and Cable Joint Stock Limited Company in 2011. He is currently a Technical Manager, responsible for the R&D of optical fibre cable (OPGW, OPPC, petroleum fibre optic cable).

Feng Chen graduated in Mechanical and Electrical Engineering from Northeast University in 1998. He joined the Yangtze Optical Fibre and Cable Joint Stock Limited Company in 2000, engaging in cable production process control. Currently, he is the General Manager of Yangtze (Hubei) Electrical Power Cable Limited Company, a subsidiary Company of YOFC.

1 Introduction

Optical fibre composite overhead ground wire (OPGW) is a special optical cable which integrates the functions of communication line and overhead ground wire. It uses the unique primary power line resources of power system to form communication network. Moreover, it has the dual functions of ground wire and optical cable. On the one hand, it serves as a shielding wire and lightning protection wire of transmission lines, which provides shielding protection for transmission lines against lightning flash discharge, plays a shielding role when the transmission lines are short-circuited, and reduces the mutual interference between the power grid and the communication network caused by short-circuit current. On the other hand, through the optical fibre compounded in the ground wire, it can transmit audio, video, data and various control signals for multi-channel broadband communication. OPGW communication line is suitable for erecting on transmission lines of 110 kV and above, realising optical cable ring network, and providing a transmission channel with good quality and high reliability for the establishment of SDH communication network (Wang et al., 2021).

In the industrial field, flexible automation manufacturing is becoming a promising solution to meet the growing demand for multi variety and small batch production, representing the future trend of industrial automation. In order to achieve flexible automated manufacturing, robots typically need to be deployed together with additional sensors, so that they can adapt to various rapidly iterating product configurations. Despite rapid development in the field of robotics in recent years, OPGW fibre optic cable insulation units centred around robots still face significant challenges (Jiang et al., 2021).

In fibre optic communication technology, Ethernet passive optical network (EPON) is widely used in the communication field due to its advantages in technology and security reliability. In power system communication, EPON technology is gradually being promoted and applied in areas such as distribution network automation, centralised meter reading, and power broadband access. In response to the communication needs of online inspection of transmission lines, EPON technology is introduced into the field of transmission networks, and combined with OPGW fibre optic connection and down lead technology (hereinafter referred to as OPGW optoelectronic separation interface technology); it makes it possible to connect any tower, which has a certain degree of foresight and innovation. In depth research on the application of EPON technology in the online inspection system of transmission lines, in order to adapt to different line conditions, is expected to achieve good application prospects. Given the widespread use of OPGW in high-voltage transmission lines, it is of great significance to study the distribution of power frequency short-circuit current in the ground wire tower grounding system of transmission lines. Flashover tripping accidents at transmission line towers caused by lightning strikes, insulator contamination, and other factors often occur. In order to ensure the safe and stable operation of the power system, combined with the analysis of the distribution of short-circuit current on OPGW, accurate positioning of transmission line fault towers is crucial to ensure the stable operation of the power system.

This paper aims to integrate machine vision into intelligent robots to realise the automatic separation of insulated optical units of OPGW optical cables. This paper combines improved machine vision to construct a three-dimensional spatial model of OPGW optical cable, combines three-dimensional measurement technology to identify the insulated optical unit from the optical cable structure, and cooperates with robot mechanical terminal to realise the accurate separation of the insulated optical unit of OPGW optical cable. Through the research in this paper, the reliability of automatic separation of insulated optical units of OPGW optical cable is further improved. At the same time, this technology can also be extended to the construction of smart grid to improve the reliability of power grid monitoring.

The organisational structure of this article is as follows: Section 1 is the introduction, which mainly describes the current application status and background of OPGW, and elaborates on the necessity of automatic separation of OPGW fibre optic cable insulation units. It also explains the research content and innovation points of this article. Section 2 is related work. It mainly studies the research status of automatic separation of OPGW optical cable insulating optical unit, describes the shortcomings of traditional research, and compares the progressiveness of this model. Section 3 is the construction of the visual algorithm model in this article, and the construction of the wire stripping robot system Section 4 is the experimental part, which verifies the performance of the automatic separation robot system in this paper. Section 5 is the conclusion section, which mainly summarises the research results of this article.

2 Related work

Many studies on cable operation focus on using the mechanical structure and operating environment of the gripper to constrain the cable. These constraint techniques aim to achieve precise operations by controlling the shape and position of the cable, thereby improving the flexibility and operational efficiency of the gripper.

Kim et al. (2020) used a designed end effectors to clamp the cable on the desktop and operated two robotic arms to adjust the position and posture of the cable. A gripper with rollers and springs was designed to grip and track cables of different sizes. A force sensor is also implemented on the gripper to help real-time correct the tracking direction of the cable by detecting the direction of force.

Zeng et al. (2021) designed a mechanical gripper for connector assembly operations. The gripper is equipped with sensors such as gripping force sensor, proximity sensor, and attitude detection sensor. The proximity sensor is used to detect the distance between the gripper and the reference plane, the gripping force sensor is used for force feedback control during the assembly process, and the attitude detection sensor is used to obtain the pose information of the connector after it is grabbed.

Shi et al. (2022) proposes an automatic cable assembly system, which includes three parts: cable automatic feeding, cable grabbing, and cable assembly. In the paper, a cone like slope is used to achieve automatic alignment of the cable after feeding, which is convenient for the robotic arm to grasp. The robotic arm gripper also uses limiters and pulleys to fix the cable pose, and the position of the connector head is marked for visual inspection. Impedance control and tilting strategy are adopted during the assembly process to achieve smooth contact motion and minimise errors in position and direction.

Kim et al. (2022) proposes a pneumatic parallel finger gripper with local adaptability. The robot first uses a camera installed on the gripper base to recognise the plane, cables, and other electronic devices and estimate their pose. Then use the soft gripping mechanism of the gripper to grip the cable. At this time, the roller installed at the fingertips rolls the cable until the cable plug reaches the fingertip position. Finally, the robotic arm plans the motion trajectory and inserts the plug into the corresponding socket.

Nguyen et al. (2022) designed a parallel gripper mechanism for passive alignment of ribbon cables. Firstly, a four link mechanism is used to fix the flat surface of the ribbon cable. Then, a conveyor belt and a worm are used to provide frictional force along the x and y directions of the plane until the ribbon cable reach the position of the limit plate, achieving passive alignment.

The method of using visual sensors to obtain cable position and posture information, and combining it with robotic arms to achieve precise control, has also received much attention. Boschetti et al. (2021) proposes a geometric modelling method for a linear flexible soft body based on two projected plane curves under gravity, which is used to track the pose of the top and gripping points of the linear flexible soft body. After the RGB-D camera captures the depth information and image information of the cable, it can obtain the pose information of the top of the cable and the selected grasping point through geometric modelling algorithm processing. Then, the robotic arm inserts the top of the cable into the designated position based on the obtained pose information.

Idà et al. (2020) proposes a cable 3D shape estimation algorithm based on 2D images to plan an appropriate grasping posture. By analysing the 2D image information of the cable from different perspectives, the 3D posture of the cable is estimated. Robots can use the cable posture provided by this algorithm to grasp cables in controlled positions.

They obtained the top position and posture information of the cable to be assembled through this algorithm in 2022, achieving the operation of inserting the cable into the designated socket.

Due to the ability of tactile sensors to accurately measure the magnitude and direction of force, research on the use of tactile sensors in cable operations is gradually emerging. Feng and Zhang (2021) designed a tactile sensor to obtain information on the position and direction of the captured cable. The sensor is divided into two layers, the outer layer is composed of flexible materials, and the inner layer is a layer of PCB board. Light reflector blocks are evenly distributed on the PCB board. In the article, finite element analysis is used to process the data of tactile sensors, and three-dimensional reconstruction is performed on cables to obtain their position and direction information. Canali et al. (2022) proposes a high-resolution tactile vision sensor for robot fingers. The sensor consists of gel, LEDs, mirror, camera and other components. The gel surface is covered with a layer of fabric to improve the durability of gel. When the object is in contact with the fabric on the surface of the gel, the gel interacts with the glancing light to produce a pattern of interlaced light spots and dark spots. The pattern was then captured by the camera through the front glass mirror. A calibration framework was also created to reduce the impact of wear on the accuracy of gel during use.

Hu et al. (2020) designed a gripper equipped with a camera and tactile sensor for the assembly of wires in narrow spaces. Convolutional neural networks were used to process visual and tactile information, completing the recognition, position, and pose estimation of wires, providing data support for robots to grasp wires

Mechanical constraints can also be applied to one end of the cable. Wang et al. (2020) proposes a solution to the challenges faced by robots when operating with tools connected by wires or ropes. They used a tool balancer to straighten the tool cable to solve the cable deformation problem, developed a planner to predict the cable state during the operation process, and used it to limit the robot's movement to avoid entanglement and collision with the cable. At the same time, they also applied the planner to generate directional constraints to limit cable bending, reducing the torque and stress borne by the robot due to cable tension.

Adding a robotic arm to improve operational flexibility is also a solution. Ageed et al. (2021) proposes a planner for operating a dual arm robot with cable tools. This planner generates a robot motion sequence (OMMS) to manipulate tools and place them in the desired position. Secondly, the planner checks the movement of tools related to OMMS and calculates candidate positions for cable sliders to manipulate the cable to avoid collisions with tools, robotic arms, or surrounding objects. This method can avoid entanglement between the robot and the cable, allowing the robotic arm to move the tool to the designated position. Yu et al. (2020) introduces a four arm robot system for collaboration, in which one main control dual arm robot operates a tool with cables by assisting the dual arm robot. The auxiliary robot helps the main control robot complete tasks such as tool placement and re grasping by manipulating cables and avoiding collisions with the surrounding environment, thereby improving the flexibility of the system. Improvements have been made to the previously used dual arm system, which required the robotic arm to relinquish control over cables in order to perform tool handover (Kim et al., 2020).

The research in the field of cable operation both domestically and internationally mainly focuses on how to determine the hand posture of cable plugs. At present, there are four main methods for determining the hand posture of cable plugs, which are tactile

based, visual based, visual tactile based, and mechanical limiting methods. The method based on visual touch is currently a hot research topic, mainly using the three-dimensional tactile sensor GelSight to obtain the three-dimensional state of the plug at the fingertips. However, after grasping the plug, its posture cannot be adjusted. If the grasped plug posture is not suitable for subsequent assembly operations, the plug can only be released and regrasped (Huang, 2020). GelSight's fingertips are covered with silicone, which is a deformable object. After grabbing the plug, the force received by the plug during assembly is offset by the silicone and cannot be transmitted to the end of the robotic arm. Therefore, traditional force control cannot be used for plug assembly (Zainuddin et al., 2020). The visual based method mainly uses image information to reconstruct the shape of the cable in 3D, and estimates the pose information of the cable based on the reconstructed 3D model. However, its disadvantage is that the imaging quality of the depth camera is greatly affected by the environment, and operating in a strong light environment may lead to the failure of 3D reconstruction (Chen, 2020). The method of mechanical positioning restricts the cable to the fixed position of the clamp through the mechanical structure, and usually passively aligns the cable. Then, the attitude information of the plug can be obtained through a visual detection algorithm based on template matching. Its disadvantage lies in the requirement for the shape of the cable to be operated on (Teimourzadeh et al., 2021).

Although the development of power operation robots in distribution networks has made significant progress, and the design of corresponding wire stripper structures has also emerged one after another, there are more or less problems of wire core damage and insulation residue accumulation on the surface of wire core during the stripping process of drainage wires and main high-voltage wires in the power operation of distribution networks, which seriously affects the distribution effect. It can be seen that relying on structures is difficult to fundamentally solve the problem of distribution quality.

This article focuses on the problem of poor distribution quality and serious impact on power supply caused by the stripping of the insulation layer of wires during the operation of power robots in distribution networks, which leads to damage to the wire core and retention of insulation residue. A terminal wire stripping robot system integrating infrared vision recognition technology is designed, and a wire stripping control algorithm based on impedance control and cutting force tracking suitable for terminal wire strippers is proposed to improve the distribution quality of distribution robots.

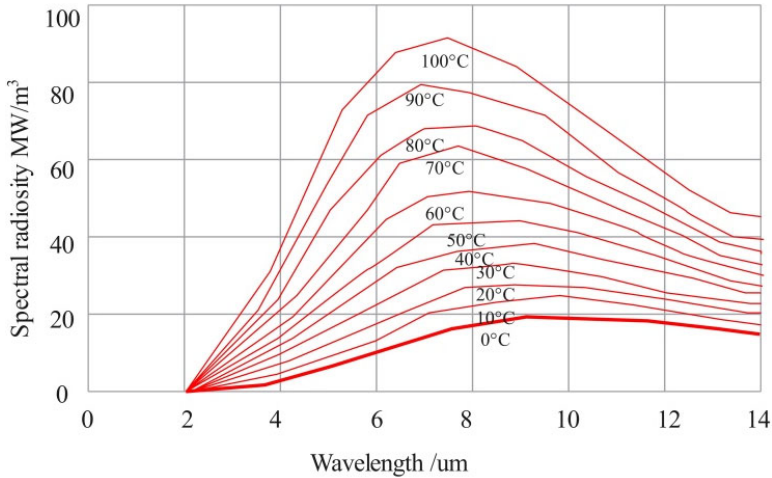
3 Model construction

3.1 Machine vision algorithm

Because the imaging principles of infrared images and visible images are different, the expression effect and functional application of images have their own characteristics. Among them, infrared images can obtain the thermal radiation of objects in the scene when the line of sight is blocked, and visible light images can reflect the detailed information of things in the scene. Therefore, fusing infrared and visible images can obtain new images with more features and richness. Nowadays, infrared and visible image fusion technology has been widely used in military, industry, remote sensing and other fields. Using image fusion technology to separate the insulation layer of OPGW optical cable insulation unit has the advantages of high efficiency and low error rate.

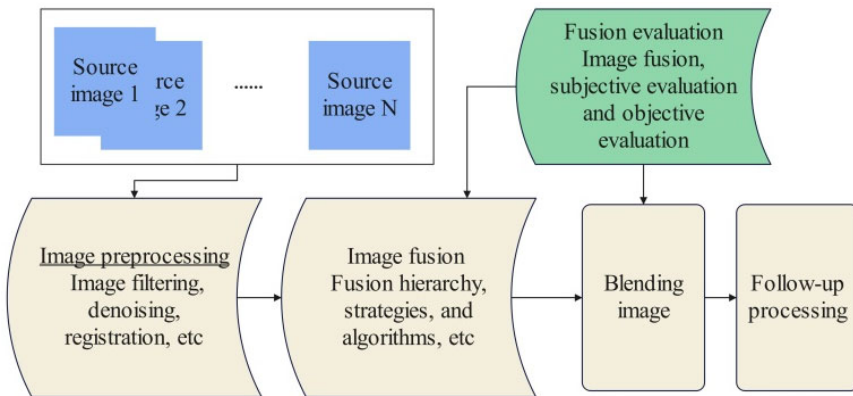
Infrared ray belongs to the electromagnetic wave band that is imperceptible to the human eye. Any object higher than thermodynamic zero in the scene will never stop emitting infrared thermal radiation to the outside world. The higher the temperature of the target object, the greater the infrared thermal radiation energy emitted outward. The spectral radiance of the blackbody at different temperatures is shown in Figure 1.

Figure 1 Blackbody spectral radiance at different temperatures (see online version for colours)



The infrared imaging sensor acquires the infrared thermal radiation of the target object in the scene and converts it into grey information, and finally converts it into infrared image. Through the obtained infrared image, the temperature of the target object can be measured non-destructively, and the temperature distribution of the target object can be analysed efficiently and accurately. When the temperature difference between the target object and the scene increases, the contrast of the infrared image also increases.

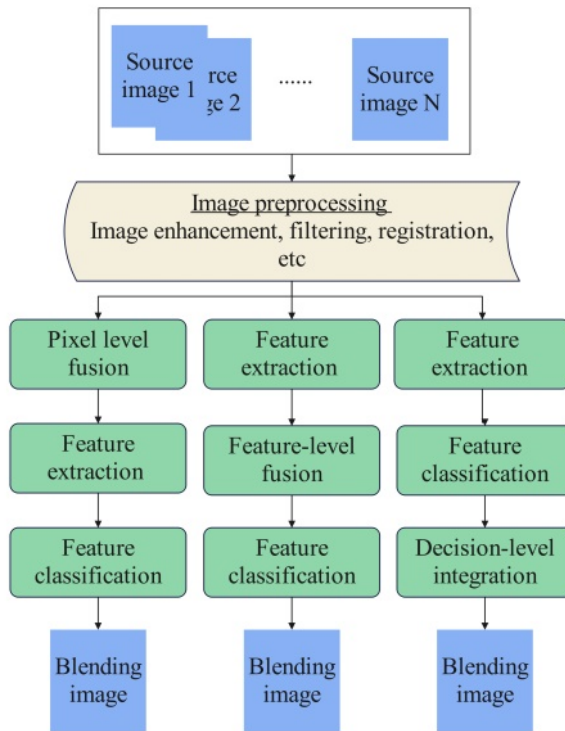
Figure 2 Schematic diagram of image fusion flow (see online version for colours)



Visible light belongs to the electromagnetic wave band that the human visual system can perceive. When there is sufficient sunlight or artificial light source in the scene, the object

absorbs part of the electromagnetic wave and reflects the complementary colour segment of the absorbed electromagnetic wave. The colour perceived by the human eye or camera is the complementary colour segment reflected by the object. In daily production and life, light sources are very important to the visible light imaging process. Among them, sunlight sources mainly include red, orange, yellow, green, blue, indigo, and purple visible electromagnetic wave bands. The visible light imaging sensor acquires the visible light electromagnetic wave band reflected by the target object in the scene and converts it into grey information, and finally converts it into visible light image. Through the obtained visible light image, the detailed information of the target object can be obtained, such as pose information, texture information, etc. Therefore, the obtained visible light image has the characteristics of high contrast and rich information expression ability.

Figure 3 Schematic diagram of image fusion framework at different levels (see online version for colours)



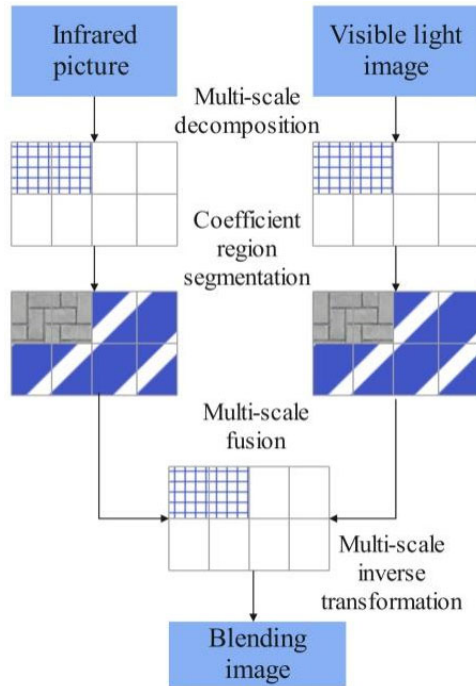
The image fusion process is shown in Figure 2, which can be roughly divided into three parts: image pre-processing, image fusion and image evaluation. The image pre-processing part includes the enhancement, filtering and registration of the source image, the image fusion part is the process of generating the fused image through a suitable fusion algorithm, and the image evaluation part is to evaluate the image quality subjectively and objectively after the fusion result.

The framework of image fusion methods at different levels is shown in Figure 3.

In image fusion tasks, image fusion algorithms based on multi-scale analysis are widely used. The main steps of the algorithm are as follows: firstly, the acquired infrared

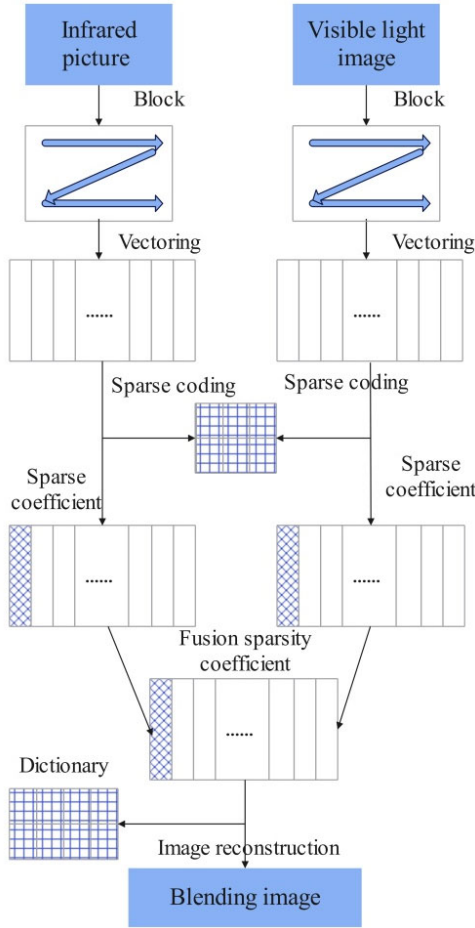
and visible images are decomposed into a series of sub-images with different frequencies and directions, that is, multi-scale sub-images (multi-scale decomposition). Next, the multi-scale sub-images corresponding to the two images are selected according to the actual situation, and fused according to the level and direction (fusion processing). Finally, the fused multi-scale sub-images are subjected to multi-scale inverse transformation to realise image fusion (image reconstruction). The algorithm framework is shown in Figure 4.

Figure 4 Image fusion framework diagram based on multi-scale analysis (see online version for colours)



Sparse representation of signals has been widely used in various practical research fields, and this method is also an effective method to express different scene images. The image fusion algorithm based on multi-scale transformation analysis aims to study the characteristics of different scales of the target object, and the theoretical core of the image fusion algorithm based on sparse representation is to represent the source image with sparse coefficients through the trained over-complete dictionary. The main steps of the algorithm are as follows: firstly, the acquired infrared and visible images are divided into image blocks from left to right and top to bottom through sliding window (block vectorisation), and then an over-complete dictionary is trained from a large number of images, and then each image block is sparsely coded. This step can obtain the sparse coefficients of two images at the same time (sparse coding). Next, appropriate fusion rules are used to fuse the sparse coefficients of the two images (coefficient fusion), and finally, the fused coefficients are combined with the over-complete dictionary to reconstruct the fused image (image reconstruction). The algorithm framework is shown in Figure 5.

Figure 5 Image fusion framework diagram based on sparse representation (see online version for colours)



Taking an infrared image as an example, the infrared image is divided into image blocks and then vectorised and expressed as a matrix Y , which is linearly expressed by an over-complete dictionary D and a sparse matrix X :

$$Y = \sum_{i=1}^k d_i x_i = DX \text{ s.t. } \min \|X\|_0 \tag{1}$$

In the formula, d_i and x_i are the atoms (column vectors) of the over-complete dictionary and the atoms (row vectors) of the sparse matrix, respectively, and formula (1) can be simplified as:

$$\min \sum_{i=1}^k \|x_i\|_0 \text{ s.t. } Y = DX \tag{2}$$

In practical applications, images will be disturbed by uncertain factors, so the formula (2) can be optimised as:

$$\min \sum_{i=1}^k \|x_i\|_0 \text{ s.t. } \|Y - DX\|_2^2 \leq \epsilon \quad (3)$$

The training of over-complete dictionary and sparse matrix is the key step of image fusion algorithm based on sparse representation. Commonly used training methods for over-complete dictionary include DCT, PCA, MOD, K-SVD and other algorithms, and commonly used training methods for sparse matrix include MP, OMP and other algorithms. The following briefly introduces the process of training overcomplete dictionaries and sparse matrices through K-SVD and OMP algorithms.

Firstly, the algorithm is initialised so that the initial residual value E_0 is equal to the vectorised representation matrix Y of the infrared image. The initial dictionary $D^{(0)}$ can be composed of selecting k column vectors in matrix Y or the first k column vectors of the left singular matrix of the singular value decomposition of matrix Y . The algorithm finds the atom with the largest absolute value of the inner product with the initial residual value E_0 from the initial dictionary $D^{(0)}$, which is denoted as $d_1^{(0)T}$, then the new residual can be expressed as:

$$E_1 = E_0 - d_1^{(0)} \left(d_1^{(0)T} d_1^{(0)} \right)^{-1} d_1^{(0)T} E_0 \quad (4)$$

At this time, the corresponding initial sparsity coefficient is:

$$x_1 = \left(d_1^{(0)T} d_1^{(0)} \right)^{-1} d_1^{(0)T} Y \quad (5)$$

From formula (5), the residual error of continuous iteration can be obtained:

$$E_{k+1} = \left(I - A_k^{(0)} \left(A_k^{(0)T} A_k^{(0)} \right)^{-1} A_k^{(0)T} \right) E_k \quad (6)$$

In the formula, the matrix I represents the identity matrix, and $A_k^{(0)}$ represents the matrix composed of atoms $d_1^{(0)}$ to $d_k^{(0)}$ as column vectors. At this time, the corresponding sparse matrix can be expressed as:

$$X = \left(A_k^{(0)T} A_k^{(0)} \right)^{-1} A_k^{(0)T} Y \quad (7)$$

The training method of sparse matrix is finished, and the next step is to train the complete dictionary by formula (3) and singular value decomposition method. After simple transformation, formula (3) can be expressed as:

$$\|Y - DX\|_2^2 = \left\| \left(Y - \sum_{i=1}^{k-1} d_i x_i \right) - d_k x_k \right\|_2^2 = \|E_k - d_k x_k\|_2^2 \quad (8)$$

In formula (8), the zero elements corresponding to the sparse coefficient vector is eliminated, and the corresponding column vector in the residual matrix is also eliminated to form a partial residual matrix, and formula (8) is transformed into:

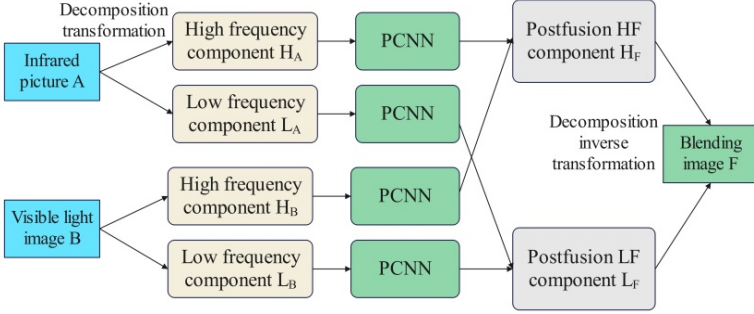
$$\min \|Y - DX\|_2^2 = \min \|E'_k - d_k x'_k\|_2^2 \quad (9)$$

By performing singular value decomposition on the partial residual matrix, the following expression can be obtained:

$$E'_k = U \sum V^T \tag{10}$$

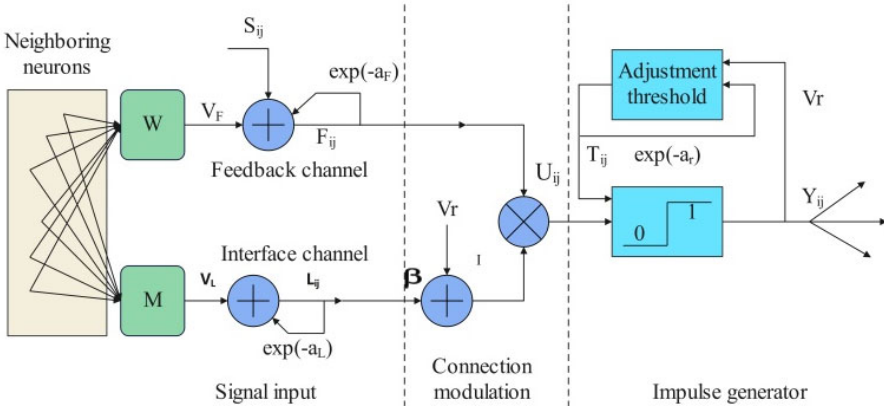
Theoretical models based on physiological inspiration are often combined with image fusion algorithms based on multi-scale transformation analysis. The algorithm framework is shown in Figure 6.

Figure 6 Image fusion framework diagram based on PCNN (see online version for colours)



In the PCNN model, each pixel of infrared and visible light images can be regarded as a neuron and connected to its neighbouring neurons. Each neuron is mainly divided into three parts: input part, modulation part and pulse generator. The basic structure of the neuron is shown in Figure 7.

Figure 7 PCNN neuron structure diagram (see online version for colours)



In the fusion of infrared and visible light images, the working process of neurons is that when the image enters the PCNN, the input part will generate two excitations F_{ij} and L_{ij} of the feedback channel and the connection channel, which are expressed as:

$$F_{ij}(n) = e^{-\alpha F} F_{ij}(n-1) + V_F \sum_{k,l} W_{ijkl} Y_{kl}(n-1) + S_{ij} \tag{11}$$

$$L_{ij}(n) = e^{-\alpha_F} L_{ij}(n-1) + V_F \sum_{k,l} M_{ijkl} Y_{kl}(n-1) \quad (12)$$

In the formula, α_F and α_L respectively represent the attenuation factor of the excitation of the feedback receiving domain and the coupling link domain and the attenuation speed of the two excitations of the control input part, V_F and V_L respectively represent the amplification factor of the signal of the feedback receiving domain and the coupling link domain, W_{ijkl} and M_{ijkl} respectively represent the weight matrix of the feedback receiving domain and the coupling link domain, and S_{ij} represents the external excitation of the feedback receiving domain. The modulation section performs a connection modulation operation on the received two excitations to obtain an internal activity term U_{ij} in the form of product coupling, which is expressed as:

$$U_{ij}(n) = F_{ij}(n)[1 + \beta L_{ij}(n)] \quad (13)$$

In the formula, β represents the link factor of the internal activity item, which is used to adjust the influence degree of incentive.

When the internal activity term reaches the threshold, the pulse generator triggers the pulse, which is called neuron ignition. On the contrary, when the internal activity term does not reach the threshold, the neuron does not perform ignition operation. The process is expressed as:

$$Y_{ij} = \begin{cases} 1 & U_{ij}(n) \geq \theta_{ij}(n) \\ 0 & U_{ij}(n) < \theta_{ij}(n) \end{cases} \quad (14)$$

3.2 Wire stripping robot system

Due to the complexity of the working environment of the distribution robot, two situations often occur during the stripping process of the wire stripper:

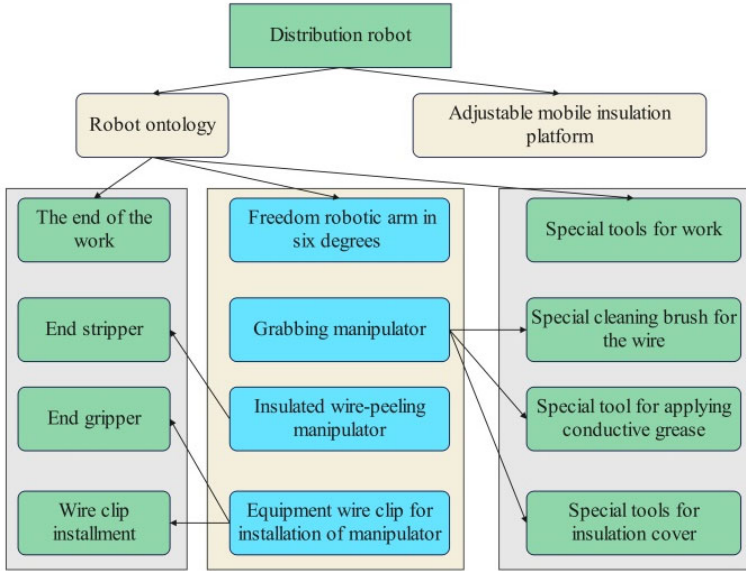
- 1 Because of the structural factors of the wire stripper itself or the poor stability of stripping motion control, the surface of the wire will be incomplete due to insufficient strength, that is, there will still be insulation residue retained on the surface of the wire.
- 2 Due to the excessive force of the stripper during the stripping process, not only the surface insulation layer of the wire is cut off, but also the metal core structure of the inner layer of the wire is damaged.

Both situations will cause immeasurable losses to subsequent power distribution situations.

After the manipulator 2 completes stripping the wire, after being controlled by the robot platform, the manipulator 1 clamps the special cleaning tool for the distribution network close to the exposed part of the stripped wire, and cleans the residual foreign matter on the surface of the wire core. After cleaning, the manipulator 1 changes its position and posture away from the wire to complete the cleaning. This process needs to be completed with the help of hand-eye calibration vision algorithm. After the wire is cleaned, the manipulator 1 sends the cleaning tool back to the platform toolbox and at the same time picks up the special tool for coating conductive grease from the toolbox to coat grease on the exposed part of the peeled wire, which is beneficial to the transmission of

electric energy. Finally, the manipulator 1 sends the special tool for coating conductive grease back to the toolbox, clamps the equipment clamp at the same time, cooperates with the manipulator 3 (installing the manipulator), fixes the wire clamp on the exposed part of the peeled main high-voltage wire, and clamps the peeled drainage wire in the clamp to complete the parallel connection between the main high-voltage wire and the drainage wire. The whole operation structure is shown in Figure 8, and this series of operation processes are completed by the cooperation of multiple manipulators, which is mainly realised by master-slave control technology.

Figure 8 Schematic diagram of operation structure (see online version for colours)

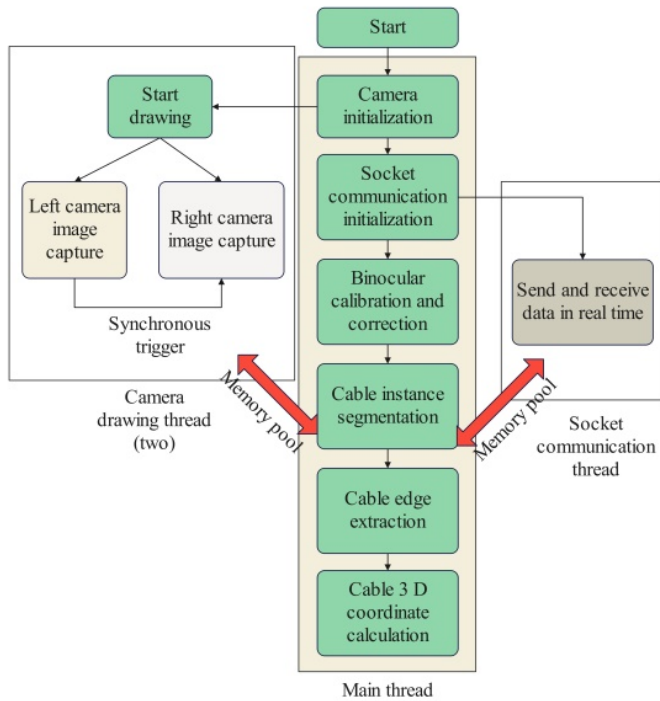


The structure of the robot hand in this paper uses the image fusion algorithm in the previous part to identify the insulation unit of OPGW optical cable. The cable 3D measurement system is divided into two parts, namely the robot end and the man-machine interaction end. The robot end mainly realises camera control, calibration and correction of vision system, cable instance segmentation and cable 3D calculation. The man-machine interaction end is mainly used for the interactive control of the robot cable 3D measurement, mainly including image display and control interface. The robot end and the man-machine interaction end are isolated through wireless network through Socket communication based on TCP protocol, so that the system operator can remotely control the robot to measure the three-dimensional coordinates of the cable to ensure the safety of the system operator. The implementation methods of the robot end and the man-machine interaction end are as follows (Figure 9):

When the wire stripper slowly approaches the wire, the wire clamping motor reverses to drive the wire clamp block (quasi-nut) structure to align the guide hole with the wire, and then rotates forward to clamp the wire. After that, the model imposes a rigid fixed constraint on the wire, and imposes a corresponding kinematic pair constraint on the internal transmission structure in the wire stripper, and defines a sensor1 module between the internal wire stripping tool and the wire. After defining the contact conditions

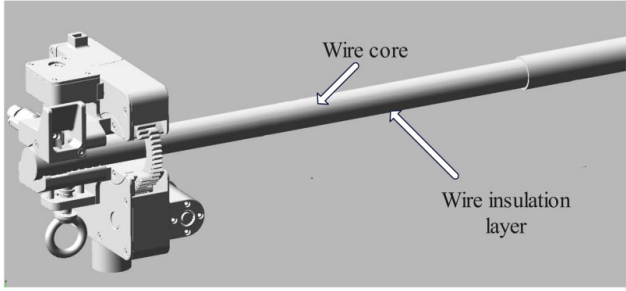
between the tool and the wire, it measures the force changes before, during and during the contact between the tool and the wire, that is, records the change of stripping and cutting force during the change of environmental stiffness. Then, it also defines a sensor2 module between the quasi-screw rod and the wire clamp blocks, defines the conditions for the clamp block to clamping the wire and relax and recover, and analyses the force change of the screw rod during the process of clamping the wire by the clamping motor. Then, the model applies a moving pair and a rotating pair along the axial direction of the wire to the overall structure of the stripper, and finally adds a driving torque. After the stripping movement is completed, the model is shown in Figure 10.

Figure 9 Implementation method of robot end (see online version for colours)



4G is a commonly used communication method for long-distance wireless communication applications. 4G technology has the advantages of good compatibility, high data transmission quality, and wide coverage. In today's consumer market where 5G technology is not yet fully popularised, 4G communication still holds a dominant position. 4G technology is widely used in industrial control, water conservancy industry, smart home, power industry, etc. 4G technology is also approaching maturity. 4G DTU is a wireless transmission module based on 4G network with high speed and low latency. In this article, the 4G DTU module model ATK-M751 is selected for transmission. System processing through this model can effectively improve system stability, reduce system latency, and improve the reliability of robot operation to a certain extent.

Figure 10 Results after stripping motion

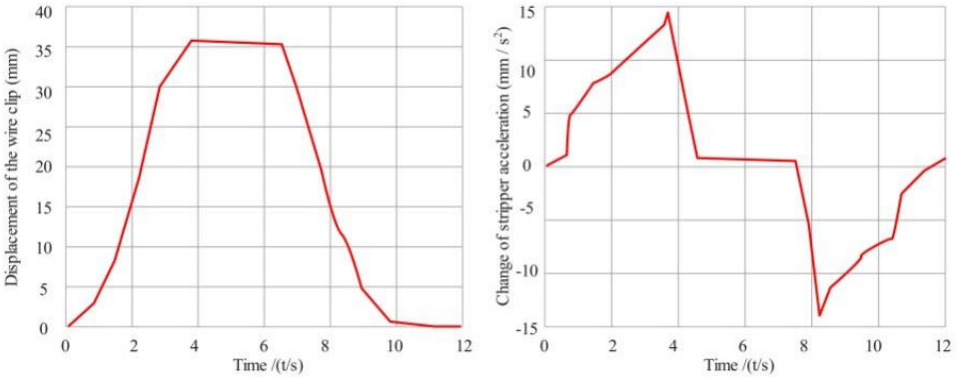


4 System simulation

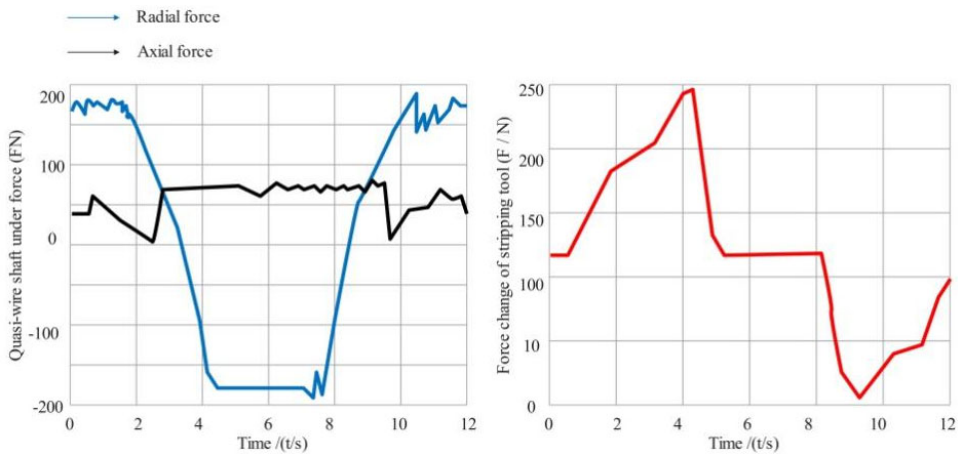
4.1 Experimental results

After all kinds of constraints and drives are applied to the wire stripper, it is simulated. The wire stripper starts to contact and clamp the wire until the wire stripper is stripped, and then the structure of the quasi-screw rod is reversed to release the wire for reset. The simulation time of this process is 13 s (the stripper stripping process is 4 s). In the process of analysing the model prototype, the displacement change of the wire clamp block, the acceleration change of the wire stripper (axial direction of the wire), the force change of the quasi-screw rod and the force change during the contact between the tool and the wire during the wire stripping process are mainly analysed, and the simulation curves shown in Figures 11 and 12 can be obtained respectively.

Figure 11 Displacement variation of clamp block and acceleration variation of stripper (see online version for colours)



The error between the manipulator and the corresponding corner point is measured, and the Euclidean error distance between the manipulator and the corresponding corner point is shown in Table 1.

Figure 12 Force change of screw rod and force change of cutter (see online version for colours)**Table 1** Manipulator finger pointing results

Distance (m)	Number	Maximum error (mm)	Mean error (mm)	Mean square error (mm)
1	1	0.40	0.34	0.05
	2	0.38	0.30	0.07
	3	0.39	0.33	0.09
0.9	1	0.33	0.27	0.05
	2	0.32	0.25	0.06
	3	0.30	0.29	0.06
0.8	1	0.25	0.21	0.02
	2	0.23	0.19	0.03
	3	0.21	0.18	0.03

MATLAB Robotic Toolbox is used to simulate and verify the kinematics model of the above robot. When the end position is at the specified speed, starting point and target position, the plane trajectory line moving from T1 to T2 position is shown in Figure 13(a), and when the end position is at the specified speed, starting point and target position, the plane trajectory line moving from T2 to T3 position is shown in Figure 13(b).

When the end start position, middle point and end position are at the specified speed, start point and target position, the spatial trajectory of moving from T1 to T3 through T2 is shown in Figure 14.

To further investigate the effectiveness of our model, we compared it with Jiang et al. (2021), Zeng et al. (2021), Shi et al. (2022), Feng and Zhang (2021), and Canali et al. (2022), calculated the systematic errors of these models, and evaluated their cable stripping effect through subjective evaluation. The experimental results are shown in Table 2.

Figure 13 Position plane trajectory line, (a) planar trajectory planning 1, (b) planar trajectory planning 2 (see online version for colours)

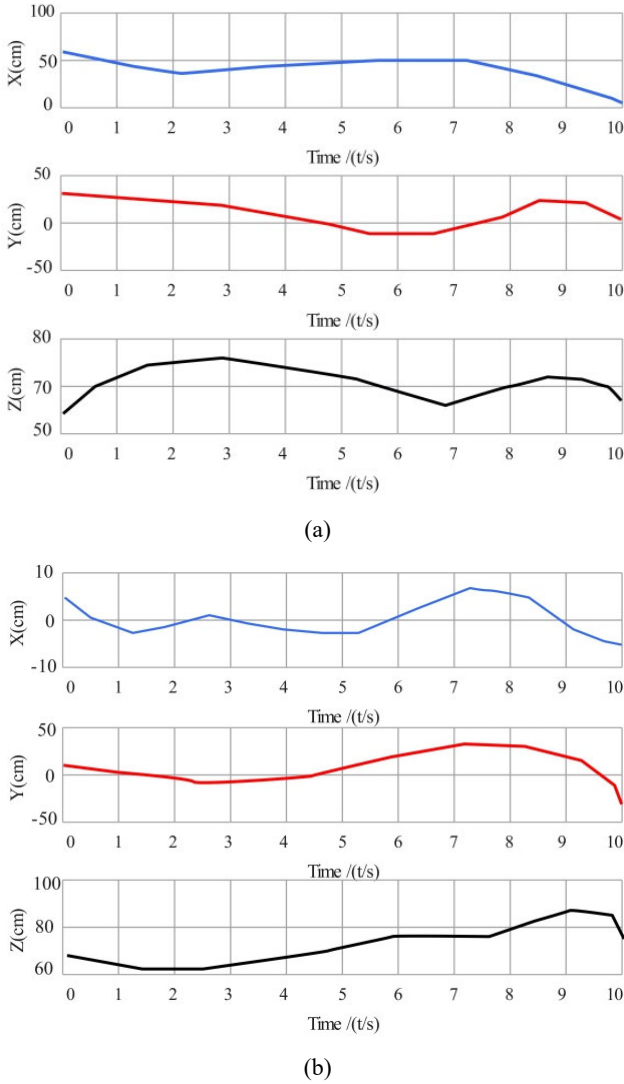
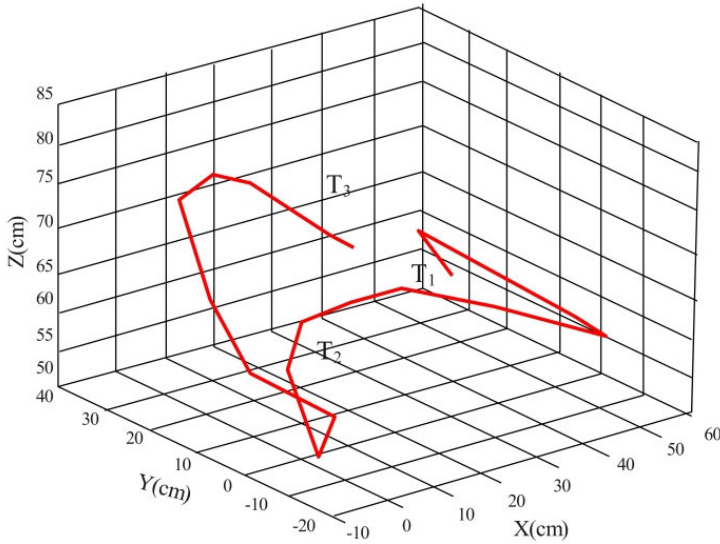


Table 2 Model comparison and evaluation

	<i>This article's model</i>	<i>Jiang et al. (2021) model</i>	<i>Zeng et al. (2021) model</i>	<i>Shi et al. (2022) model</i>	<i>Feng and Zhang (2021) model</i>	<i>Canali et al. (2022) model</i>
System error (mm)	0.43	1.67	0.49	0.58	0.61	0.78
Peel off effect	88.74	75.38	78.22	84.19	84.82	78.14

Figure 14 Trajectory planning of spatial end (see online version for colours)

4.2 Analysis and discussion

It can be seen from Figure 11 that during the stripping process of the wire stripper, the wire clamp block is reset from opening to clamping the wire to finally loosening the wire. The displacement curve in Figure 11 basically reflects this process. During the wire stripping process, the wire stripper cutter accelerates from fast to slow from the beginning of contacting the wire to slowly cutting into the wire. When it is about to touch the internal wire core, it keeps a certain force and cuts at a constant speed until the wire insulation layer is peeled off, and then the wire stripper loosens the wire. The process of this stripping movement can be said to be almost symmetrical, as shown in Figure 11.

In the process of wire stripper cutting the wire, the stress of the quasi-screw nut mechanism is also the focus of analysis. In the above chapter, we made a static analysis of the screw nut structure, and the rated axial load is 200 N and the rated radial load is 90 N. After the simulation of wire stripping motion in Adams, the stress of the quasi-screw in Figure 12 is obtained. The radial load and axial maximum load are within the rated load, which illustrates the feasibility of this method and structural design from the side. Moreover, during the stripping process of the wire stripper, the contact force of the tool basically changes linearly with time, until the insulating layer is completely cut, and the tool rotates and cuts with constant force. After the cutting is completed, the wire stripper is separated from the wire, and the contact force of the tool is gradually reduced to zero. The simulation data in Figure 12 is just consistent with the theoretical analysis.

As shown in Table 1, from the results of manipulator finger pointing, the finger pointing error is positively correlated with the placement distance of the checkerboard. With the increase of finger pointing distance, the finger pointing error also increases, but the error is less than 0.4 mm between 0.08 mm and 0.1 mm. It shows that under the condition of accurate matching of the left and right cameras, the finger pointing accuracy of the manipulator guided by the three-dimensional coordinates measured by this binocular system reaches 0.4 mm.

Traditional models often rely on image recognition to determine cable units, which can be affected by various external factors such as lighting, unit spacing, etc. which can affect the robot's cable recognition results. This article uses the Hongai recognition technology to effectively eliminate the effects of lighting, positioning, and unit spacing, thereby improving the system's accuracy.

The wire stripping robot in this article only needs to work in the external environment during operation, mostly indoors. Therefore, the system in this article only requires simple maintenance after operation, and does not require long-term high-frequency maintenance.

From the estimated motion results in Figure 13 and Figure 14, it can be seen that the robot system for automatic separation of insulated optical units of OPGW optical cable combined with machine vision proposed in this paper can cope with complex motions under complex conditions and is suitable for the actual needs of automatic separation of insulated optical units of OPGW optical cable.

From the comparative analysis in Table 2, it can be seen that the model proposed in this paper has higher system accuracy, and the accuracy of other models is also higher, but it is difficult to meet the requirements of cable insulation layer stripping. Secondly, in subjective evaluation, the evaluation result of this paper is the highest, indicating that the model proposed in this paper has higher working effect compared to traditional models.

5 Conclusions

This paper combines experiments to verify the effect of the robot system for automatic separation of insulated optical units of OPGW optical cable. The experimental results show that the operation effect of the system is very remarkable, the three-dimensional coordinate guided mechanical finger point accuracy measured by this binocular system reached 0.4mm, and the maximum radial and axial loads of the tool were within the rated load, which indirectly demonstrates the feasibility of this method and structural design. The robot system designed in this article reduces the damage to the metal layer of cables caused by traditional methods, lowers the risk of cable stripping, and improves the automated visual inspection effect of cables in harsh environments. It also provides automation reference for more complex cable operations in the future.

Although this article has developed an OPGW fibre optic cable insulation light unit automatic separation robot system based on the fusion of infrared and visible light images, the warning function in the software design of this article is not comprehensive enough. In the future, more warning functions will be added, such as fault line selection based on the warning area, sound alarm, warning light flashing, automatic SMS alarm sending, etc. to further improve the effectiveness of warning.

The infrared image sensor used in this paper needs to rely on interpolation algorithms to smooth the imaging, so the visual effect of the imaging needs to be improved. In the future, infrared image sensors with better imaging effects will be used for research, which is also the follow-up research direction.

Acknowledgements

State Grid Corporation of China Science and Technology Project Funding (Contract No. kj2023-043).

References

- Ageed, Z.S., Zeebaree, S.R., Sadeeq, M.A., Abdulrazzaq, M.B., Salim, B.W., Salih, A.A. and Ahmed, A.M. (2021) 'A state of art survey for intelligent energy monitoring systems', *Asian Journal of Research in Computer Science*, Vol. 8, No. 1, pp.46–61.
- Boschetti, G., Minto, R. and Trevisani, A. (2021) 'Experimental investigation of a cable robot recovery strategy', *Robotics*, Vol. 10, No. 1, pp.35–43.
- Canali, C., Pistone, A., Ludovico, D., Guardiani, P., Gagliardi, R., De Mari Casareto Dal Verme, L. and Caldwell, D.G. (2022) 'Design of a novel long-reach cable-driven hyper-redundant snake-like manipulator for inspection and maintenance', *Applied Sciences*, Vol. 12, No. 7, pp.3348–3360.
- Chen, W. (2020) 'Intelligent manufacturing production line data monitoring system for industrial internet of things', *Computer Communications*, Vol. 151, No. 5, pp.31–41.
- Feng, J. and Zhang, W. (2021) 'Autonomous live-line maintenance robot for a 10 kV overhead line', *IEEE Access*, Vol. 9, No. 2, pp.61819–61831.
- Hu, R., Iturralde, K., Linner, T., Zhao, C., Pan, W., Pracucci, A. and Bock, T. (2020) 'A simple framework for the cost–benefit analysis of single-task construction robots based on a case study of a cable-driven facade installation robot', *Buildings*, Vol. 11, No. 1, pp.8–18.
- Huang, X. (2020) 'Intelligent remote monitoring and manufacturing system of production line based on industrial internet of things', *Computer Communications*, Vol. 150, No. 3, pp.421–428.
- Idà, E., Marian, D. and Carricato, M. (2020) 'A deployable cable-driven parallel robot with large rotational capabilities for laser-scanning applications', *IEEE Robotics and Automation Letters*, Vol. 5, No. 3, pp.4140–4147.
- Jiang, W., Ye, G.C. and Yan, Y. (2021) 'Mechanism configuration and innovation control system design for power cable line mobile maintenance robot', *Robotica*, Vol. 39, No. 7, pp.1251–1263.
- Kim, H., Lee, H. and Kim, S.W. (2022) 'Current only-based fault diagnosis method for industrial robot control cables', *Sensors*, Vol. 22, No. 5, pp.1917–1928.
- Kim, M.C., Kim, E.S., Park, J.O., Choi, E. and Kim, C.S. (2020) 'Robotic localization based on planar cable robot and hall sensor array applied to magnetic capsule endoscope', *Sensors*, Vol. 20, No. 20, pp.5728–5740.
- Kim, S., Kim, D., Jeong, S., Ham, J.W., Lee, J.K. and Oh, K.Y. (2020) 'Fault diagnosis of power transmission lines using a UAV-mounted smart inspection system', *IEEE Access*, Vol. 8, No. 5, pp.149999–150009.
- Nguyen, K.V., Van Bach Pham, N. and Dao, T.T. (2022) 'Damage detection of cables in cable-stayed bridges using vibration data measured from climbing robot', *Advances in Structural Engineering*, Vol. 25, No. 13, pp.2705–2721.
- Shi, Y., Wang, J., Li, S., Li, B. and Sun, X. (2022) 'Tracking control of cable-driven planar robot based on discrete-time recurrent neural network with immediate discretization method', *IEEE Transactions on Industrial Informatics*, Vol. 19, No. 6, pp.7414–7423.
- Teimourzadeh, H., Moradzadeh, A., Shoaran, M., Mohammadi-Ivatloo, B. and Razzaghi, R. (2021) 'High impedance single-phase faults diagnosis in transmission lines via deep reinforcement learning of transfer functions', *IEEE Access*, Vol. 9, No. 3, pp.15796–15809.

- Wang, B., Ma, F., Ge, L., Ma, H., Wang, H. and Mohamed, M.A. (2020) 'Icing-EdgeNet: a pruning lightweight edge intelligent method of discriminative driving channel for ice thickness of transmission lines', *IEEE Transactions on Instrumentation and Measurement*, Vol. 70, No. 2, pp.1–12.
- Wang, Z., He, B., Zhou, Y., Liu, K. and Zhang, C. (2021) 'Design and implementation of a cable inspection robot for cable-stayed bridges', *Robotica*, Vol. 39, No. 8, pp.1417–1433.
- Yu, L., Nazir, B. and Wang, Y. (2020) 'Intelligent power monitoring of building equipment based on internet of things technology', *Computer Communications*, Vol. 157, No. 3, pp.76–84.
- Zainuddin, N.M., Rahman, M.A., Kadir, M.A., Ali, N.N., Ali, Z., Osman, M. and Nasir, N.M. (2020) 'Review of thermal stress and condition monitoring technologies for overhead transmission lines: issues and challenges', *IEEE Access*, Vol. 8, No. 1, pp.120053–120081.
- Zeng, P., He, J. and Gao, B. (2021) 'Reliable robot-flock-based monitoring system design via a mobile wireless sensor network', *IEEE Access*, Vol. 9, No. 2, pp.47125–47135.